

Finite optical Hamiltonian systems

Kurt Bernardo Wolf^a, Natig M. Atakishiyev^b, Luis Edgar Vicent^{c,†}, Guillermo Krötzsch^a and Juvenal Rueda-Paz^d

^aInstituto de Ciencias Físicas, Universidad Nacional Autónoma de México;

^bInstituto de Matemáticas, Universidad Nacional Autónoma de México;

^cCICATA–IPN Unidad Altamira, Instituto Politécnico Nacional;

^dFacultad de Ciencias, Universidad Autónoma del Estado de Morelos
Av. Universidad s/n, Cuernavaca, Mor. 62210, Mexico

ABSTRACT

In this essay we *finitely quantize* the Hamiltonian system of geometric optics to a finite system that is also Hamiltonian, but where signals are described by complex N -vectors, which are subject to unitary transformations that form the group $U(N)$. This group can be decomposed into $U(2)$ -paraxial and aberration transformations. Proper irreducible representation bases are thus provided by quantum angular momentum theory. For one-dimensional systems we have waveguide models. For two-dimensional systems we can have Cartesian or polar sensor arrays, where digital images are subject to unitary rotation, gyration or asymmetric Fourier transformations, as well as a unitary map between the two arrays.

Keywords: Finite optical models, signal analysis, phase space

1. INTRODUCTION: FINITE QUANTIZATION

Geometric optics is a continuous, classical Hamiltonian system which can be *finitely quantized* into a Hamiltonian system that is finite and consists of $N \times N$ self-adjoint matrices. This process is similar to—but distinct from—the usual Schrödinger quantization of classical mechanics. The finite quantization of optics yields models that apply in finite signal analysis and pixellated image processing. There is general interest in finite systems because their states—signals—represent the input data that is sampled with finite (nanoscale¹) sensor arrays, and thereafter handled by digital computation. Our approach is based on group-theoretical models where the tools of symmetry are used to define appropriate orthonormal bases for the space of signals, and to understand their phase space. In this essay we review the group-theoretical formulation of these systems, relating results for the paraxial and metaxial régimes, in one and two dimensions. Most references will thus cite works of our group.

Plane geometric optics in a medium of refractive index $n(x, z)$ is a Hamiltonian system whose phase space (x, p) at a standard screen line ($z = \text{constant}$) has a position coordinate $x \in \mathfrak{R}$, and a momentum coordinate $p = n(x, z) \sin \theta$, $\theta \in \mathcal{S}^1$ (the circle). In segments of z -homogeneous media, the Hamiltonian functions we consider have the generic form

$$h(x, p) := -\sqrt{n(x)^2 - p^2} \approx \frac{1}{2}p^2/\nu_0 - n_2(x) + \dots \quad (1)$$

In the paraxial régime, one extends phase space to $(x, p) \in \mathfrak{R}^2$, $n(x) \approx n_2(x) := \nu_0 - \nu_1 x - \nu_2 x^2$, bringing the system in contact with the classical systems of quadratic potentials $-n_2(x)$. The standard harmonic waveguide or oscillator has the Hamiltonian $h = \frac{1}{2}(p^2 + x^2)$, and the Hamilton equations of this model (using Poisson brackets) are

$$\{x, p\} := 1, \quad \{h, x\} = -p, \quad \{h, p\} = x, \quad (2)$$

while 1 Poisson-commutes with x, p, h . These are a basis for the one-dimensional oscillator algebra osc_1 . The Schrödinger quantization of this algebra on the Hilbert space $\mathcal{L}^2(\mathfrak{R})$ is well known. The Hamiltonian is the only compact generator of the algebra, which thus has a discrete albeit infinite (lower-bound) spectrum.

Further author information: (Send correspondence to Kurt Bernardo Wolf)
bwolf@fis.unam.mx; phone 52 777 317-3388

† Deceased.

We *deform* the oscillator algebra (2) to the unitary algebra $\mathfrak{u}(2) = \mathfrak{u}(1) \oplus \mathfrak{su}(2)$, where the three generators of $\mathfrak{su}(2) = \mathfrak{so}(3)$ have discrete and finite spectra $\{-j, -j+1, \dots, j\}$ in any one of its irreducible representations of integer dimension $N = 2j + 1$. This replaces osc_1 in (2) with commutators of matrices

$$[\mathbf{X}, \mathbf{P}] := -i\mathbf{K}, \quad [\mathbf{K}, \mathbf{X}] = -i\mathbf{P}, \quad [\mathbf{K}, \mathbf{P}] = i\mathbf{X}, \quad (3)$$

and $\mathbf{1} \in \mathfrak{u}(1)$ commuting with all, on the complex N -vector space \mathbb{C}^N . In this representation, the operators are $N \times N$ self-adjoint matrices

$$X_{m,m'} = m \delta_{m,m'}, \quad m, m' \in \{-j, -j+1, \dots, j\}, \quad (4)$$

$$P_{m,m'} = -i\frac{1}{2}\sqrt{(j-m)(j+m+1)}\delta_{m+1,m'} + i\frac{1}{2}\sqrt{(j+m)(j-m+1)}\delta_{m-1,m'}, \quad (5)$$

$$K_{m,m'} = \frac{1}{2}\sqrt{(j-m)(j+m+1)}\delta_{m+1,m'} + \frac{1}{2}\sqrt{(j+m)(j-m+1)}\delta_{m-1,m'}. \quad (6)$$

Here the position operator \mathbf{X} in (4) is diagonal, the momentum operator \mathbf{P} in (5) is a purely imaginary skew-symmetric weighted central difference matrix, while \mathbf{K} in (6) is real and symmetric; we call the latter the *pseudo-Hamiltonian*, since it is related to the ‘true’ Hamiltonian of the finite oscillator by

$$\mathbf{H}_{\text{osc}} := \mathbf{K} + (j + \frac{1}{2})\mathbf{1}. \quad (7)$$

These matrices are bound by the Casimir invariant $\mathbf{C} := \mathbf{X}^2 + \mathbf{P}^2 + \mathbf{K}^2 = j(j+1)\mathbf{1}$.

This compactification of the paraxial optical model is, in a nutshell, the finite quantization process. The Casimir invariance implies that phase space, previously flat, becomes a sphere of radius $\sqrt{j(j+1)}$. The classical sphere is of course a symplectic manifold, and in Sec. 2 we justify that the finitely quantized phase space can be treated in the same way as the Schrödinger-quantized phase space through the introduction of an $\text{SU}(2)$ -covariant Wigner function. In Sec. 3 we recall the finite oscillator functions and coherent states, which are the actors in one-dimensional systems. Sec. 4 condenses developments on the separation between $\text{SU}(2)$ -linear transformations and $\text{U}(N)$ aberrations in N -point systems. Following considerations on the convergence of the aberration series, in Sec. 5, we treat the ‘exact’ quantization of the waveguide Hamiltonian (1), which is the square root of a positive matrix, and where the two root signs represent forward- and backward-moving finite wavefields in the guide. In Sec. 6 we succinctly report on current research on two-dimensional finite systems, whose states are images pixellated along Cartesian and along polar coordinates. The concluding remarks in Sec. 7 address the context of some further lines of work.

2. THE $\text{SU}(2)$ PHASE SPACE AND WIGNER FUNCTION

The Wigner function used in standard paraxial wave optics² can be defined by asking for the covariance between a classical function and a quantum operator function. The classical function is $F_c(\xi, \eta; x, p) := \exp[-i(\xi x + \eta p)]$, built with the observables of position and momentum $(x, p) \in \mathfrak{R}^2$; this generates translations by $(\eta, -\xi)$ of phase space under Poisson brackets. Including the phases generated by 1, this is the general element of the Heisenberg-Weyl (HW) subalgebra of the oscillator algebra $\mathfrak{hw}_1 \subset \text{osc}_1$. The quantum operator function is $\widehat{F}_Q(\xi, \eta) := \exp[-i(\xi \widehat{X} + \eta \widehat{P})]$, with the Schrödinger operators of position \widehat{X} and momentum \widehat{P} , which also generates translations on their linear space. The standard HW-Wigner *operator* is then obtained as the bilinear generating function which integrates over the translation parameters,

$$\widehat{W}_{\text{HW}}(x, p) := \iint_{\mathfrak{R}^2} d\xi d\eta F_c(x, p; \xi, \eta)^* \widehat{F}_Q(\xi, \eta). \quad (8)$$

Finally, the expectation value of this operator in a quantum state $\psi(x)$ is the well-known Wigner function $W_{\text{HW}}(\psi|x, p) := \langle \psi | \widehat{W}_{\text{HW}}(x, p) | \psi \rangle$ used in quantum mechanics and in paraxial wave optics.

Applying the same strategy to arbitrary groups whose generators correspond to classical observables x, p, κ in $\mathcal{G} := \text{SU}(2)$ or its \mathcal{Z}_2 -quotient $\text{SO}(3)$, we introduce a *classical* function on the \mathfrak{R}^3 algebra manifold^{3,4}

$$G_c[u, v, w; x, p, \kappa] := \exp[-i(ux + vp + w\kappa)], \quad \begin{cases} u = \rho \sin \theta \sin \phi, \\ v = \rho \sin \theta \cos \phi, \\ w = \rho \cos \theta, \end{cases} \quad (9)$$

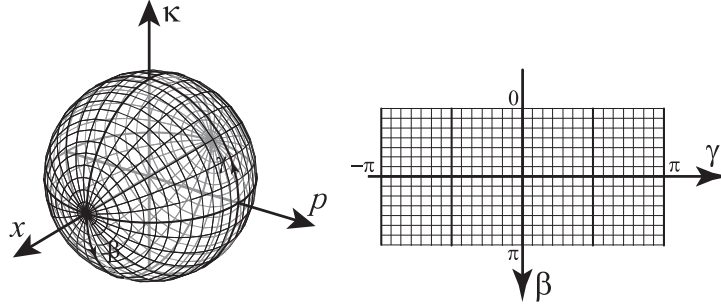


Figure 1. *Left:* Polar coordinates of the sphere $(\beta, \gamma) \in \mathcal{S}^2$ referred to the x -axis of positions. *Right:* Projection of the sphere onto the rectangle $\beta|_0^\pi, \gamma|_{-\pi}^\pi$. Both the sphere and the rectangle are divided into octants by heavy lines.

where $[x, p, \kappa] \in \mathfrak{R}^3$ are the Cartesian coordinates of *meta*-phase space. The coordinates on the group are $[u, v, w] \equiv (\rho, \theta, \phi) \in \mathcal{S}^3 = \text{SU}(2)$, with ranges $\rho|_0^{4\pi}$ for $\text{SU}(2)$ or $\rho|_0^{2\pi}$ for $\text{SO}(3)$, and $(\theta|_0^\pi, \phi|_{-\pi}^\pi) \in \mathcal{S}^2$. We ask for covariance with an *operator* function on the group \mathcal{G} ,

$$\mathbf{G}(\rho, \theta, \phi) \equiv \mathbf{G}[u, v, w] := \exp[-i(u\mathbf{X} + v\mathbf{P} + w\mathbf{K})]. \quad (10)$$

This $N \times N$ unitary matrix is a Wigner *Big-D* matrix⁵ that carries the action of $\text{SU}(2)$ on N -point vectors of ‘spin’ j (for $N = 2j+1$).^{6–9}

Covariance between (9) and (10) is built through the bilinear generating function, which integrates over the group manifold of \mathcal{G} , and yields the unitary, self-adjoint ‘Wigner matrix’

$$\begin{aligned} \mathbf{W}[x, p, \kappa] &\equiv \mathbf{W}(r, \beta, \gamma) \\ &:= \int_{\mathcal{G}} d^{\text{H}}[u, v, w] G_c[u, v, w; x, p, \kappa]^* \mathbf{G}[u, v, w] \end{aligned} \quad (11)$$

$$= \int_{\mathcal{G}} d^{\text{H}}[u, v, w] \exp i[u(x-\mathbf{X}) + v(p-\mathbf{P}) + w(\kappa-\mathbf{K})], \quad (12)$$

where we use the spherical coordinates of \mathfrak{R}^3 meta-phase space $x = r \cos \beta$, $p = r \sin \beta \sin \gamma$, and $\kappa = r \sin \beta \cos \gamma$, and the \mathcal{G} -invariant Haar measure $d^{\text{H}}[u, v, w] := du dv dw = \rho^2 d\rho \sin \theta d\theta d\phi =: d^{\text{H}}(\rho, \theta, \phi)$.

Finally, the \mathcal{G} -Wigner *function* of the signal N -vector $\mathbf{f} = \{f_m\}_{m=-j}^j$ is the expectation value of (12) in that state, $W(\mathbf{f} | r, \beta, \gamma) := \mathbf{f}^\dagger \mathbf{W}(r, \beta, \gamma) \mathbf{f}$. This can be factorized as $W_j(r) W(\mathbf{f} | \beta, \gamma)$, where $W_j(r)$ is a function of the radius that has significant positive values only for $r \approx \sqrt{j(j+1)}$, and

$$W(\mathbf{f} | \beta, \gamma) = \sum_{m, m'=-j}^j f_m^* W_{m, m'}(\beta, \gamma) f_{m'}, \quad (13)$$

$$W_{m, m'}(\beta, \gamma) = e^{-i(m-m')\gamma} \sum_{\bar{m}=-j}^j d_{m, \bar{m}}^j(\beta) \bar{W}_{\bar{m}}^j d_{\bar{m}, m'}^j(-\beta). \quad (14)$$

The sphere $(\beta, \gamma) \in \mathcal{S}^2$ is thus the proper phase space for finite Hamiltonian systems.³ All the angular dependence of the matrix $\|W_{m, m'}(\beta, \gamma)\|$ in (13) is thus contained in the Wigner little- d matrices, and there only remains the diagonal ‘sub-Wigner’ matrix $\|\delta_{m, m'} \bar{W}_{m'}^j\|$ in (14) to be computed for any given dimension N . This has an analytic expression³ but can be conveniently computed.¹⁰

Because we have *position* as the diagonal operator, the x -axis takes the role of the traditional “ z -pole.” And since the broadest features of a signal occur for low energies $\kappa \approx -r$, where the sphere is tangent to the classical phase space plane $(x, p) \in \mathfrak{R}^2$, it is convenient to project the sphere onto the rectangle $\beta|_0^\pi, \gamma|_{-\pi}^\pi$, as shown in Fig. 1, where the center of rectangle is the point of tangency of the finite and continuous phase spaces. In Fig. 2 we show the $\text{SO}(3)$ -Wigner function of a finite rectangle signal.

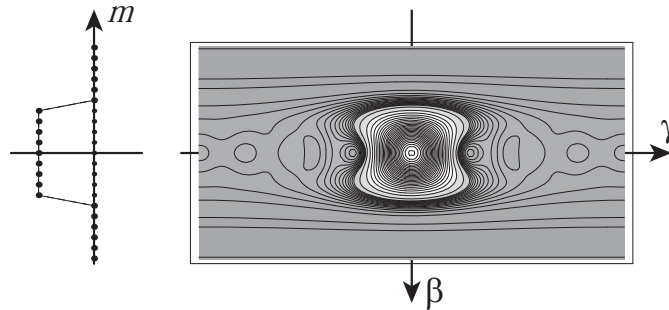


Figure 2. *Left:* A ‘rectangle’ signal $R(m)$ on $N = 21$ points ($j = 10$) that has value 1 for $|m| \leq 5$ and zero elsewhere. *Right:* The $\text{SO}(3)$ Wigner function of this signal, $W(\mathbf{R}|\beta, \gamma)$.

3. FINITE OSCILLATOR AND COHERENT STATES

The finite analogues of the quantum harmonic oscillator wavefunctions are the overlaps between the natural Kronecker eigenvectors of the diagonal position matrix \mathbf{X} in (4), $|x_m\rangle_1$ with $x_m \equiv m|_j^j$, and the eigenbasis of pseudo-energy \mathbf{K} in (6), $|n\rangle_3$, where we use the *number* label $n = \kappa - j|_0^{2j}$. These overlaps between eigenfunctions of two generators of rotations whose axes are separated by $\frac{1}{2}\pi$ rotation, are Wigner *little-d* functions⁵

$$\Psi_n(x_m) := \langle x_m | n \rangle_3 = d_{n-j, m}^j(\frac{1}{2}\pi) = \Psi_{m+j}(n-j) \quad (15)$$

$$= \frac{(-1)^n}{2^j} \sqrt{\binom{2j}{n} \binom{2j}{m+j}} K_n(m+j; \frac{1}{2}, 2j). \quad (16)$$

In the last expression we have the square root of a binomial as a finite a Gaussian) and a Kravchuk polynomial, finite analogue of the Hermite ones.¹¹ In⁶ we called (16) the *Kravchuk functions*; we thus have an orthonormal and complete real basis for complex N -point signals.

Coherent states of the finite oscillator are defined, as in the standard theory, to be meta-phase space rotations of the oscillator ground state $\Psi_0(x_m)$. Through rotations by $\theta|_0^\pi$ around the momentum axis, we have the family of coherent states

$$\Upsilon_\theta^j(x_m) := \sum_{m'=-j}^j \left(\exp(i\theta\mathbf{P}) \right)_{m, m'} \Phi_0^j(x_{m'}) = d_{-j, m}^j(\frac{1}{2}\pi + \theta), \quad (17)$$

where the little- d function can take any angle. Further rotation around the vertical evolution axis will assign a coherent state to every point on the sphere, as shown schematically in Figure 3.

4. PARAXIAL TRANSFORMATIONS AND ABERRATIONS

The finite quantization process can be applied to optical models beyond the linear $\text{SO}(3)$ transformations. Nonlinear transformations of the classical phase space plane $(x, p) \in \mathfrak{R}^2$ are generated by the Poisson operators $M_0^{k, m}(x, p) := \{p^{k+m} x^{k-m}, \circ\}$, said to be aberrations of rank $k \in \{0, \frac{1}{2}, 1, \frac{3}{2}, \dots\}$ and weight $m \in \{k, k-1, \dots, -k\}$,¹² [13, Chap. 13]. When the symplectic manifold is a sphere $x^2 + p^2 + \kappa^2 = \text{constant}$, we can use $\text{so}(3)$ Berezin brackets, which have all the properties of Poisson brackets, but on the three coordinates $(x, p, \kappa) \in \mathfrak{R}^3$, and are defined by the basic ones: $\{x, p\}_B = \kappa$, $\{p, \kappa\}_B = x$, and $\{\kappa, x\}_B = p$. The generators of all transformations of the sphere will be the Berezin operators $\{x^a p^b \kappa^c, \circ\}_B$, which belong to an infinite-dimensional Lie algebra, graded by their *rank* $a + b + c = 2k$. For $2k = 1$ they generate rigid rotations of the sphere; and for $k > 1$ they generate nonlinear transformations of its surface, preserving Berezin brackets and volume elements in meta-phase space.

The finite quantization of the monomial functions $x^a p^b \kappa^c$ with *Weyl ordering* yields $N \times N$ self-adjoint matrices, of which there are N^2 independent ones that close into the Lie algebra $\mathfrak{u}(N)$ that generates the Lie group

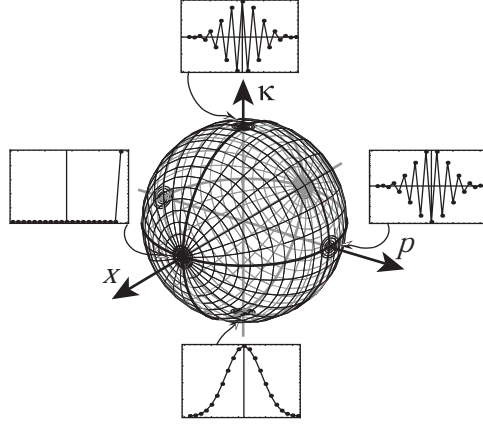


Figure 3. The sphere of finite ($N = 21$, $j = 10$) coherent states $\Upsilon_{\theta,\phi}(x_m)$, obtained from phase space rotations of the ground state $\Upsilon_{0,0}(x_m) = \Psi_0(x_m)$ at the bottom pole. The state $\Upsilon_{\pi/2,0}(x_m)$ along the x -axis is the extreme Kronecker state at $x_j \equiv j$; the $\frac{1}{2}\pi$ harmonic evolution leads to $\Upsilon_{\pi/2,\pi/2}(x_m)$ along the p -axis. The top coherent state reproduces the ground state with a change of sign between consecutive points.

$U(N)$. They are graded into multiplets of $2k + 1$ aberrations for each rank $k \in \{0, \frac{1}{2}, 1, \dots\}$. We proposed in Ref.¹⁰ the monomial basis of matrices

$$\mathbf{M}_0^{k,m}(\mathbf{X}, \mathbf{P}) := \{\mathbf{P}^{k+m} \mathbf{X}^{k-m}\}_{\text{Weyl}}, \quad m \in \{-k, -k+1, \dots, k\}, \quad (18)$$

$$\mathbf{M}_1^{k,m}(\mathbf{X}, \mathbf{P}, \mathbf{K}) := \{\mathbf{K} \mathbf{M}^{k-1/2,m,0}(\mathbf{X}, \mathbf{P})\}_{\text{Weyl}}, \quad m \in \{-k+\frac{1}{2}, -k+\frac{3}{2}, \dots, k-\frac{1}{2}\}, \quad (19)$$

where the Casimir condition prevents the appearance of powers of \mathbf{K} higher than 1. The singlet $\mathbf{M}_0^{0,0} = \mathbf{1}$ generates overall phases $U(1) \subset U(N)$, and the triplet $\{\mathbf{M}_0^{1,1}, \mathbf{M}_1^{1/2,0}, \mathbf{M}_0^{1,-1}\}$ generate the $SO(3)$ -linear rigid rotations of the sphere. Thereafter, $\mathbf{M}_0^{k,m}$ and $\mathbf{M}_1^{k,m}$, generate flow lines at the bottom pole of the sphere in Fig. 1 which are tangent to the classical flows of $\{\mathbf{M}_0^{k,m}, \circ\}$ aberrations. For $|m| < k$, the $\mathbf{M}_0^{k,m}$ flows loop within quadrants, while the $\mathbf{M}_1^{k,m}$ flows are inside octants, because of the extra factor of κ . In Ref.¹⁰ we illustrated these deformations of phase space for aberrations up to rank $k = 3$, with the intention to mimic the transformation of geometric optical beams and images on N -point signals or $N \times N$ pixellated screens, using the aberration coefficients computed for the former in Ref. [13, Chap. 14].

5. PLANAR WAVEGUIDE HAMILTONIANS

We considered waveguides whose Hamiltonian is (1), and instead of approximating the square root by a slow-converging aberration series, we considered the square root form directly for a family of *elliptic* refractive index profiles, $[n^{\nu,\mu}(x)]^2 = \nu^2 - \mu^2 x^2$, for $|x| < \nu/\mu$. Taking the Casimir into account, the finitely quantized Hamiltonian matrix is

$$\mathbf{H}^{\nu,\mu} = -\sqrt{\nu^2 \mathbf{C} - \mathbf{P}^2 - \mu^2 \mathbf{X}^2} = -\sqrt{[(\nu^2-1)\mathbf{C} - (\mu^2-1)\mathbf{X}^2] + \mathbf{K}^2}. \quad (20)$$

Noting that for $\nu = 1 = \mu$, (20) is $\mathbf{H} = -\sqrt{\mathbf{K}^2}$, this case serves as reference when we let the parameters ν, μ depart into the generic elliptic profile; a second parametric anchor is the free case $\mu = 0$.

The eigenvectors of the $(\mathbf{H}^{1,1})^2$ are the Kravchuk functions $\Psi_n(x_m)$ in (16), and its eigenvalues are $\lambda^{1,1} := \kappa^2 |j^2|$ (from κ_{-j}^j), forming j doublets and a ground singlet; in the free case, $(\mathbf{H}^{1,0})^2$ also has j doublets but a *top* singlet. Within that μ -interval the eigenvalues $\eta^{\nu,\mu}$ of $\mathbf{H}^{\nu,\mu}$ are nondegenerate, but we have to identify the \pm signs of their square root. With the eigenvector matrix $\Psi := \|\Psi_{\eta_n}(x_m)\|$ we solve

$$\begin{aligned} (\mathbf{H}^{\nu,\mu})^2 \Psi_{\eta}(m) &= \lambda^{\nu,\mu} \Psi_{\eta}(m), & \lambda^{\nu,\mu} &:= (\eta^{\nu,\mu})^2 \geq 0, \\ \Psi^\dagger (\mathbf{H}^{\nu,\mu})^2 \Psi &= \Lambda^{\nu,\mu}, & \Psi &= \|\Psi_{\eta_n}(m)\| \\ \Lambda^{\nu,\mu} &= \text{diag}(\lambda_{\max}^{\nu,\mu}, \lambda_{\max-1}^{\nu,\mu}, \dots, \lambda_{\min+1}^{\nu,\mu}, \lambda_{\min}^{\nu,\mu}). \end{aligned} \quad (21)$$

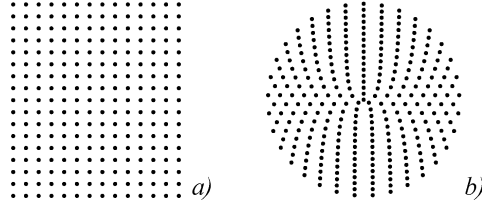


Figure 4. Two-dimensional screens for $j = 8$ ($N = 17$). a): Cartesian arrangement (m_x, m_y) . b): Polar arrangement (ρ, ϕ_k) with the same number of points.

The problem of finding the square root of a matrix is similar to that faced by Dirac to Schrödinger-quantize $E = \sqrt{(mc^2 + p^2)}$ out of a second-order differential operator. In the free case, he found four uncoupled solutions. Our problem is $SU(2)$ rather than the Lorentz group, and the system is discrete rather than continuous. But here also we can identify the forward-moving solutions by $\eta < 0$ and the backward-moving ones by $\eta > 0$.¹⁴

The eigenvectors $\Psi_\eta \equiv \Psi_\eta^{\nu, \mu}$ of $(\mathbf{H}^{\nu, \mu})^2$ in (21) satisfy a *step-2 difference* equation¹⁵ obtained from the matrices (4)–(6). It does not seem possible to find a known discrete special function to solve it exactly for general ν, μ . This step-two difference equation in fact stands for *two* difference equations: one binding $\Psi_\eta^e(m)$'s with m odd, and the other binding $\Psi_\eta^o(m)$'s with m even. When solving (21) by machine computation, the result is that the first has zeros at even m 's, and the second with zeros at odd m 's, both having a ‘porcupine’ appearance, as shown in Refs.^{14, 15} The ‘good’ eigenfunctions are obtained as the sum and difference of the right- and left-moving solutions,

$$\Psi_\eta^{\rightarrow}(m) := [\Psi_\eta^e(m) + \Psi_\eta^o(m)]/\sqrt{2} \quad \Psi_\eta^{\leftarrow}(m) := [\Psi_\eta^e(m) - \Psi_\eta^o(m)]/\sqrt{2}. \quad (22)$$

6. TWO-DIMENSIONAL FINITE SYSTEMS

We now give a brief review of the extension of the finite quantization process to Hamiltonian systems that transform two-dimensional pixellated images. It would seem that such finite images in two dimensions can only be pixellated on rectangular arrays of points, where they are direct products of two one-dimensional signals. On a square screen of side $N = 2j+1$ there will be an N^2 -dimensional space of images. However, a group-theoretical accident allows for other models, because it turns out that the direct sum of two $\mathfrak{su}(2)$ algebras is isomorphic with the Lie algebra $\mathfrak{so}(4)$ that generates rotations in a 4-dimensional space,

$$\mathfrak{su}(2)_x \oplus \mathfrak{su}(2)_y = \mathfrak{so}(4) \supset \mathfrak{so}(3)_\rho \supset \mathfrak{so}(2)_\theta. \quad (23)$$

When the representation indices of the two summand algebras are j , reduced by the position subalgebra $\mathfrak{u}(1)_x \oplus \mathfrak{u}(1)_y$ with Kronecker basis (m_x, m_y) , the $\mathfrak{so}(4)$ representation is reduced with respect to the canonical subalgebra $\mathfrak{so}(3)_r$, yielding representations $0 \leq \rho \leq 2j$ that we endow with the meaning of a radial discrete variable; each of these in turn is reduced with respect to $\mathfrak{so}(2)_\theta$ into a $2\rho+1$ -dimensional Kronecker basis of angular momenta $|m| \leq \rho$. Through the finite Fourier matrix, this turns into a set of $2\rho+1$ equidistant angles θ_k modulo 2π . The total number of points is thus $N^2 = (2j+1)^2$, the same as for the $N \times N$ square screen. In Fig. 4 we show the two screens.

This is separation of variables—for discrete and finite coordinates. The overlap between the two bases is thus a purely group-theoretic affair that we solve with Clebsch-Gordan coefficients, yielding a unitary transformation between pixellated images on one screen and on the other. In Ref.¹⁶ we have thus mapped images between both screens. We have been interested in the general problem of separation into discrete *elliptic* coordinates, following the existence of non-subgroup reductions for $\mathfrak{so}(3)$ which have continuous counterparts in the quantum harmonic oscillator,¹⁷ but this goal has not yet been achieved.

In plane geometric optics, fractional Fourier transforms form the compact subgroup $SO(2) \subset Sp(2, \mathbb{R})$; in three dimensions (where screens are planes), the compact subgroup is $U(2) \subset Sp(4, \mathbb{R})$, called the $U(2)$ -Fourier group.¹⁸ It includes fractional Fourier transforms in the x - and y -directions, rotations between the x - and y -phase space coordinates,¹⁹ and *gyrations* which cross-rotate them.²⁰ In Fig. 5 we show the relation between these transformations as rotations of the sphere. We can require that under the finite quantization process, the

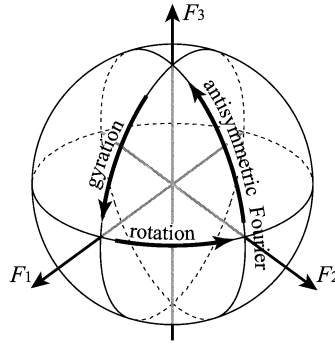


Figure 5. Action of the Fourier group $U(2)$ on the sphere. The isotropic Fourier transformation lies in the $U(1)$ center of the group.

$U(2)$ -Fourier group action on finite pixellated images be unitary and effective in either of the two arrays in Fig. 4.²¹ In this way we obtain two distinct N^2 -dimensional unitary and irreducible representations of the Fourier $U(2)$ group. These two representations are bridged by the transformation between images on both arrays.¹⁶

7. CONCLUDING REMARKS

The applications of the finite quantization process lies in the analysis and synthesis of signals and images. Square (or rectangular) sensor arrays are commonly used to assess the quality of laser beams. To find the formant modes it is common to use the sampled Hermite-Gauss or Laguerre-Gauss functions to expand the observed image. Since we have at hand the finite Kravchuk (16) and polar functions obtained by gyration, we have compared the fidelity that the sampled and the finite bases provide to reproduce a finite signal or image.^{22,23}

A complete study of the properties of Wigner functions on Lie groups and their coset spaces is still in process. The HW case was analyzed in,²⁴ the present $SO(3)$ case in³ and on a general class of Lie groups in.⁴ In the present case, the $SO(3)$ -covariant Wigner function turns out to be equivalent to the Stratonovich-Agarwal Wigner function that was built out of the irreducible tensor decomposition of wavefields, as shown in.²⁵ The analysis of discrete but *infinite* signals has been based on the noncompact Euclidean algebra $iso(2)$ in Ref.,²⁶ where phase space is a cylinder and the Hamiltonian system is free. In Refs.^{27,28} we studied the Lorentz algebra $so(2,1)$ to define discrete repulsive oscillator models, but their phase space—which ought to be hyperboloids—has not been described. All desirable properties of the standard Wigner function are present in the \mathcal{G} -Wigner function, except for the non-negativity of the ground energy state.

As this essay suggests, there are several avenues of research open in the finite optical model for signal and image processing. It seems to us that the use we have given to group theory—in particular that of $SU(2)$ traditionally used for quantum angular momentum—is a novel way to treat discrete systems that are Hamiltonian and have a phase space and Wigner function that is properly covariant.

ACKNOWLEDGEMENTS

We thank the support of the *Óptica Matemática* projects DGAPA-UNAM IN-105008 and SEP-CONACYT 79899.

REFERENCES

- [1] Papp, E. and Micu, C., [Low-dimensional nanoscale systems on discrete spaces], World Scientific, Singapore (2007).
- [2] Forbes, G. W. *et al.* Eds., [Wigner Distributions and Phase Space in Optics], Feature Issue of J. Opt. Soc. Am. A 17(12), December (2000).
- [3] Atakishiyev, N. M., Chumakov, S. M. and Wolf, K. B., “Wigner distribution function for finite systems,” J. Math. Phys. 39, 6247–6261 (1998).

- [4] Ali, S. T., Atakishiyev, N. M., Chumakov, S. M., and Wolf, K. B., “The Wigner function for general Lie groups and the wavelet transform,” *Ann. H. Poincaré* 1, 685–714 (2000).
- [5] Biedenharn, L. C. and Louck, J. D., [Angular Momentum in Quantum Mechanics], *Encyclopedia of Mathematics and its Applications*; Ed. by G.-C. Rota, Addison-Wesley (1981).
- [6] Atakishiyev, N. M. and Wolf, K. B., “Fractional Fourier-Kravchuk transform,” *J. Opt. Soc. Am. A* 14, 1467–1477 (1997).
- [7] Atakishiyev, N. M., Vicent, L. E. and Wolf, K. B., “Continuous vs. discrete fractional Fourier transforms,” *J. Comp. Appl. Math.* 107, 73–95 (1999).
- [8] Atakishiyev, N. M., Pogosyan, G. S. and Wolf, K. B., “Finite models of the oscillator,” *Phys. Part. Nuclei* 36, 521–555 (2005).
- [9] Wolf, K. B. and Krötzsch, G., “Geometry and dynamics in the fractional discrete Fourier transform,” *J. Opt. Soc. Am. A* 24, 651–658 (2007).
- [10] Wolf, K. B., “Linear transformations and aberrations in continuous and in finite systems,” *J. Phys. A* 41, art. 304026 (19 p.) (2008).
- [11] Atakishiyev, N. M. and Suslov, S. K., “Difference analogs of the harmonic oscillator,” *Theor. Math. Phys.* 85, 1055–1062 (1991).
- [12] Dragt, A. J., Forest, E. and Wolf, K. B., “Foundations of a Lie algebraic theory of geometrical optics,” in: [Lie Methods in Optics], *Lecture Notes in Physics*, Vol. 250, Springer-Verlag (1986); Chap. 4, pp. 105–158.
- [13] Wolf, K.B., [Geometric Optics on Phase Space] Springer-Verlag (2004).
- [14] Rueda-Paz, J. and Wolf, K. B., “Finite signals in planar waveguides,” *J. Opt. Soc. Am. A* 28, 641–650 (2011).
- [15] Rueda-Paz, J. and Wolf, K. B., “Optical waveguide Hamiltonians leading to step-2 difference equations,” *J. Phys. Conf. Series* 284, art. 012051 (8 p.) (2011).
- [16] Vicent, L. E. and Wolf, K. B., “Unitary transformation between Cartesian- and polar-pixelated screens,” *J. Opt. Soc. Am. A* 25, 1875–1884 (2008).
- [17] Grosche, C., Karayan, Kh. G., Pogosyan, G. S. and Sissakian, A. N., “Free motion on the three-dimensional sphere: the ellipso-cylindrical bases,” *J. Phys. A* 30, 1629–1657 (1997).
- [18] Simon, R., and Wolf, K. B., “Fractional Fourier transforms in two dimensions,” *J. Opt. Soc. Am. A* 17, 2368–2381 (2000).
- [19] Vicent, L. E., “SU(2) unitary rotation of square pixelated images,” *Appl. Math. Comput.* 221, 111–117 (2009).
- [20] Wolf, K. B. and Alieva, T., “Rotation and gyration of finite two-dimensional modes,” *J. Opt. Soc. Am. A* 25, 365–370 (2008).
- [21] Vicent, L. E., and Wolf, K. B., “The Fourier U(2) group and separation of discrete variables,” Submitted (Feb. 2011).
- [22] Wolf, K. B., “Mode analysis and signal restoration with Kravchuk functions,” *J. Opt. Soc. Am. A* 26, 509–516 (2009).
- [23] Vicent, L. E. and Wolf, K. B., “Analysis of digital images into energy-angular momentum modes,” *J. Opt. Soc. Am. A* 28, 808–814 (2011).
- [24] Wolf, K. B., “Wigner distribution function for paraxial polychromatic optics,” *Opt. Comm.* 132, 343–352 (1996).
- [25] Chumakov, S. M., Klimov, A. B. and Wolf, K. B., “On the connection of two Wigner functions for spin systems,” *Phys. Rev. A* 61, art. 034101 (3 p.) (2000).
- [26] Nieto, L. M., Atakishiyev, N. M., Chumakov, S. M., and Wolf, K. B., “Wigner distribution function for Euclidean systems,” *J. Phys. A* 31, 3875–3895 (1998).
- [27] Muñoz, C. A., Rueda-Paz, J. and Wolf, K. B., “Discrete repulsive oscillator wavefunctions,” *J. Phys. A* 42, art. 485210 (12 p.) (2009).
- [28] Wolf, K. B., “Discrete systems and signals on phase space,” *Appl. Math. & Information Science* 4, 141–181 (2010).